

Linköping Studies in Science and Technology
Licentiate Thesis No. 1357

Characterization of Ti_2AlC Coatings Deposited with High Velocity Oxy-Fuel and Magnetron Sputtering Techniques

Jenny Frodelius



Linköpings universitet
INSTITUTE OF TECHNOLOGY

LIU-TEK-LIC-2008:15
Thin Film Physics Division
Department of Physics, Chemistry, and Biology (IFM)
Linköping University
SE-581 83 Linköping, Sweden

© Jenny Frodelius 2008

ISBN: 978-91-7393-936-2

ISSN 0280-7971

Printed by LiU-Tryck, Linköping 2008

To John and my Family
for tireless support

Abstract

This Thesis presents two different deposition techniques for the synthesis of Ti_2AlC coatings. First, I have fabricated Ti_2AlC coatings by high velocity oxy-fuel (HVOF) spraying. Analysis with scanning electron microscopy (SEM) show dense coatings with thicknesses of $\sim 150 \mu\text{m}$ when spraying with a MAXTHAL 211TM Ti_2AlC powder of size $\sim 38 \mu\text{m}$ in an H_2/O_2 gas flow. The films showed good adhesion to stainless steel substrates as determined by bending tests and the hardness was 3-5 GPa. X-ray diffraction (XRD) detected minority phases of Ti_3AlC_2 , TiC , and Al_xTi_y alloys. The use of a larger powder size of $56 \mu\text{m}$ resulted in an increased amount of cracks and delaminations in the coatings. This was explained by less melted material, which is needed as a binding material. Second, magnetron sputtering of thin films was performed with a MAXTHAL 211TM Ti_2AlC compound target. Depositions were made at substrate temperatures between ambient and $1000 \text{ }^\circ\text{C}$. Elastic recoil detection analysis (ERDA) shows that the films exhibit a C composition between 42 and 52 at% which differs from the nominal composition of 25 at% for the Ti_2AlC -target. The Al content, in turn, depends on the substrate temperature as Al is likely to start to evaporate around $700 \text{ }^\circ\text{C}$. Co-sputtering with Ti target at a temperature of $700 \text{ }^\circ\text{C}$, however, yielded Ti_2AlC films with only minority contents of TiC . Thus, the addition of Ti is suggested to have two beneficial roles of balancing out excess of C and to retain Al by providing for more stoichiometric Ti_2AlC synthesis conditions. Transmission electron microscopy and X-ray pole figures show that the Ti_2AlC grains grow in two preferred orientations; epitaxial Ti_2AlC (0001) // Al_2O_3 (0001) and with 37° tilted basal planes of Ti_2AlC ($10\bar{1}7$) // Al_2O_3 (0001).

Preface

The work presented in this Licentiate Thesis is part of my PhD studies in the Thin Film Physics Division at Linköping University. The aim of my research is to generate knowledge about deposition processes for MAX-phase materials, especially the Ti-Al-C system, and their microstructure/property relationships. Parts of the work have been performed in close collaboration with Chalmers University (Göteborg), University West (Trollhättan), and Kanthal AB (Hallstahammar). I have been supported by The National Graduate School in Materials Science and the VINNEX Center FunMat.

Included Papers

Paper I **Ti₂AlC coatings deposited by High Velocity Oxy-Fuel spraying**

J. Frodelius, M. Sonestedt, S. Björklund, J.-P. Palmquist, K. Stiller,
H. Högberg, L. Hultman
Submitted for publication

Paper II **Direct current magnetron sputtering from Ti₂AlC target**

J. Frodelius, P. Eklund, M. Beckers, P.O.Å. Persson H. Högberg, L. Hultman
In manuscript

Related Papers

Magnetron sputtering of Ti₃SiC₂ thin films from a compound target

P. Eklund, M. Beckers, J. Frodelius, H. Högberg, L. Hultman
Journal of Vacuum Science and Technology A **25** (2007) 1381

Homoepitaxy of Ti-Si-C MAX-phase thin films on bulk Ti₃SiC₂ substrates

P. Eklund, A. Murugaiah, J. Emmerlich, Zs. Czigány, J. Frodelius,
M.W. Barsoum, H. Högberg, L. Hultman
Journal of Crystal Growth **304** (2007) 264

| | |
|---|-----------|
| <i>Abstract</i> | 1 |
| <i>Preface</i> | 3 |
| Included Papers | 3 |
| Related Papers | 3 |
| <i>1. Introduction</i> | 7 |
| <i>2. The Ti-Al-C system</i> | 9 |
| 2.1 Ternary MAX phases | 9 |
| 2.2 Binary phases | 11 |
| 2.2.1 TiC | 11 |
| 2.2.2 Ti-Al alloys | 12 |
| <i>3. Deposition of Thick Coatings</i> | 13 |
| 3.1 High Velocity Oxy-Fuel | 14 |
| 3.1.1 The effect of gas and powder parameters | 15 |
| 3.1.2 Structure of Thermal Sprayed Coatings | 16 |
| <i>4. Synthesis of Thin Films</i> | 17 |
| 4.1 Sputtering | 17 |
| <i>5. Plasma physics</i> | 21 |
| 5.1 Plasma breakdown | 21 |
| 5.2 Sheath | 21 |
| 5.3 Plasma analysis | 22 |
| 5.3.1 Langmuir probe | 22 |
| 5.3.2 Mass spectrometry | 23 |
| <i>6. Comments on the Results</i> | 27 |
| <i>References</i> | 29 |

Paper I

Paper II

1. Introduction

Coatings are used to improve and complement the properties of bulk materials. Examples of such properties are hardness, resistivity, oxidation resistance, and appearance. These properties, on the other hand, cannot be claimed to be good or bad unless we associated them with some sort of application. A CD disk, for instance, needs a coating that reflects the laser in a CD player, while eye-glasses can make use of an antireflective coating to provide a better visual appearance. Both of these applications, however, could make use of scratch resistant coatings to extend their lifetime. If you start to look around you will see that many products are improved by or rely on coatings.

This Thesis focuses on coatings of the MAX phase material. The MAX phases are a family of ternary carbides and nitrides that was first discovered by Nowotny [1] in the 1960's. They did not gain much attention until the 1990's when Barsoum [2] realized that the material was an intermediate between a ceramic and a metal. MAX phases have an interesting combination of properties such as thermal shock resistance [3], thermal and electrical conductivity [4] and machinability [5]. Ti_2AlC , another MAX phase member, has a desirable oxidation resistance. MAX phases have been of interest as thin films since 1972 when Nickl et al. [6] synthesized the films using chemical vapor deposition (CVD). Nowadays, the most popular technique used in the research of MAX phase thin films is magnetron sputtering. These studies were initiated at Linköping University in 2002 by Seppänen et al. [7].

This Thesis presents the synthesis and characterization of two different kinds of MAX phase Ti_2AlC coatings. In Paper I, a new deposition process for Ti_2AlC is introduced, namely high velocity oxy-fuel spraying, which is a well established family of techniques in e.g. the aerospace industry. My aim was to make Ti_2AlC available for new applications that rely on thick coatings with good mechanical and thermal properties. The project is a collaboration between Linköping University, Chalmers University, University West and Kanthal AB. The second project investigates magnetron sputtering synthesis of Ti_2AlC . The Thesis will first introduce the Ti_2AlC and other related phases of the Ti-Al-C system. Then thermal spraying and more specifically high velocity oxy-fuel is described. Finally the Thesis brings up the magnetron sputtering technique and related plasma physics.

2. The Ti-Al-C system

In this section you will be introduced to the phases in the Ti-Al-C system that this work has shown interest for. First the MAX-phases which have been the model material of my research. Second, the binary phases which in one way or another play an important role for the properties in the thin film and coatings. A phase diagram over the Ti-Al-C system is shown below to give an idea of the relation between these three elements.

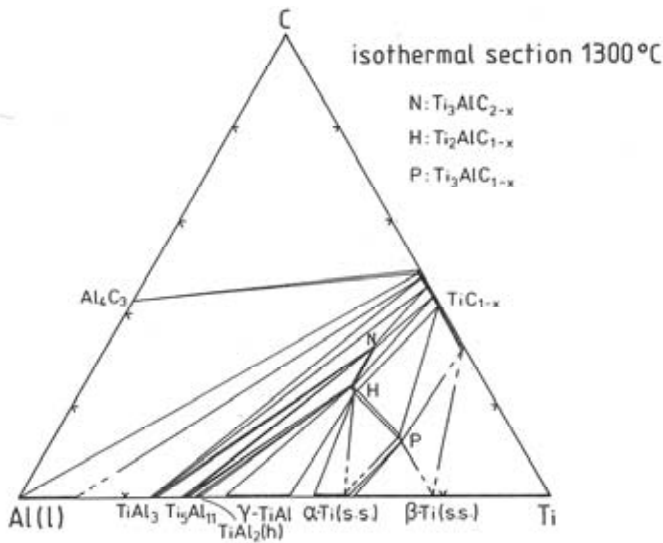


Figure 1. The ternary phase diagram for Ti-Al-C system [8].

2.1 Ternary MAX phases

There are three ternary phases within the Ti-Al-C system. Two are MAX phases, namely Ti_2AlC and Ti_3AlC_2 , and one is a perovskite, Ti_3AlC . MAX phases are a family of ternary carbides and nitrides. The name $M_{n+1}AX_n$ describes the elements included where M is a transition metal, A is an A-element and X is C or N. The stoichiometry can vary ($n = 1, 2,$ or 3) leading to 211, 312, or 413 phases. The crystal structure of Ti_2AlC and Ti_3AlC_2 is hexagonal with space group $P6_3/mmc$ and is illustrated in Figure 2. The crystals contain TiC layers interleaved with single Al layers. The stacking sequence depends on the stoichiometry where Ti_3AlC_2 , has one Al layer for every third TiC layer, and Ti_2AlC , has one Al layer for every second TiC layer. The TiC is built up by Ti octahedrons connected in each edge with C atoms filling the octahedral sites.

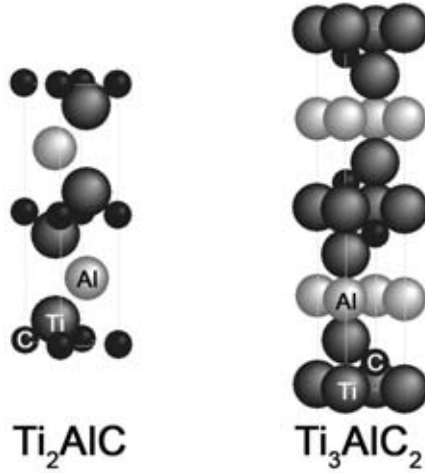


Figure 2. Crystal structure of Ti_2AlC (211) and Ti_3AlC_2 (312).

The atomic binding character in these MAX phases has been shown to be metallic, ionic and covalent [9]. The covalent-ionic Ti-C bonds are comparable to the bonds in the binary TiC and are stronger than the metallic Ti-Al bonds present in the ternary structure [10]. The relatively weak bonds between the TiC and Al layers (basal planes) contribute to an anisotropic character of the material leading to kink-band formation and delaminations along the basal planes upon deformation [11]. Due to the mix of strong TiC bonds and metallic Al-Al bonds the Ti_2AlC exhibit both ceramic and metallic properties such as low density of 4.1 g/cm^3 and good electrical conductivity ($3 \times 10^6 \Omega^{-1}\text{m}^{-1}$) [9,12]. The bulk modulus (186 GPa) is lower than for the binary TiC (450 GPa), which yields a more ductile material than the ceramic itself [10,13]. Further, Ti_2AlC exhibits excellent machinability [14] and thermal shock resistance [12]. The hardness is $\sim 5.5 \text{ GPa}$ [12] for bulk material, while for thin films its been measured to 20 GPa [15].

An interesting feature for the phases Ti_2AlC and Ti_3AlC_2 is their oxidation resistance. Research has shown that they mainly form Al_2O_3 scales in oxidizing environments. The oxide scale exhibits a high density which will slow down diffusion of more oxygen through the oxide scale to the MAX phase surface and therefore prevent further oxidation [16]. Al_2O_3 adheres very well to Ti_2AlC and does not peel off during thermal cycling even though the lattice parameters are quite different between $\alpha\text{-Al}_2\text{O}_3$ ($a = 4.76 \text{ \AA}$, $c = 12.99 \text{ \AA}$ [17]) and Ti_2AlC ($a = 3.04 \text{ \AA}$, $c = 13.6 \text{ \AA}$ [18]). The explanation is the thermal expansion coefficient of $\alpha\text{-Al}_2\text{O}_3$ [17] which is in the same range as Ti_2AlC [19].

2.2 Binary phases

2.2.1 TiC

TiC is among the hardest materials known. It has also attracted attention because of its high melting point and wear resistance. It is widely used as protective coatings for cutting, molding and milling tools, coatings for ball-bearings and spray gun nozzles as well as for fusion-reactor applications. TiC has a face-centered cubic close packed crystal structure (NaCl) and the space group is $Fm\bar{3}m$. TiC belongs to the group of interstitial carbides where carbon occupies the octahedral sites between the close packed Ti atoms – interstitial carbon, see Figure 3. Interstitial carbides has partly ionic and covalent bonds, but with a metallic character that causes a relatively low electrical resistivity of $50 \mu\Omega\text{cm}$, compared with Ti of $40 \mu\Omega\text{cm}$ [20]. The strong ionic bonds between Ti and C are due to the great difference in electronegativity of 1.0. TiC exhibits Young's Modulus of $\sim 450 \text{ GPa}$, a melting point around $3000 \text{ }^\circ\text{C}$, density of 4.9 g/cm^3 [20]. The hardness is $\sim 25 \text{ GPa}$ [21], while for TiC thin films it can be as high as $\sim 30 \text{ GPa}$ [22] due to lattice defects.

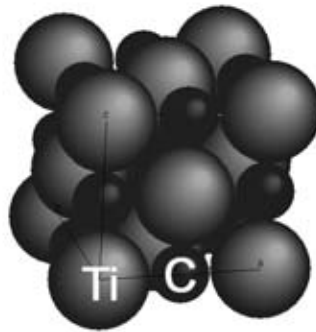


Figure 3. NaCl crystal structure of TiC with interstitial C at the octahedral sites.

The TiC is stable over a broad range of compositions. This makes TiC_{1-x} a non-stoichiometric carbide where a large amount of carbon vacancies may be present. The C content can vary between 32 and 49 at% [17]. This will cause a variation in cell parameters and consequently also variations in properties for TiC_{1-x} .

In both Paper I and Paper II TiC is a competitive phase for the synthesis of Ti_2AlC coatings.

2.2.2 Ti-Al alloys

Ti-Al alloys have a combination of properties such as low density of $\sim 4 \text{ g/cm}^3$, good creep resistance and high strength [23]. This has made them interesting as structural materials at high temperature which is useful within the aerospace and automotive industry. The phase diagram below, Figure 4, shows the different Ti-Al phases from Ti-rich Ti_3Al to TiAl to Al-rich Al_3Ti . Ti_3Al has a hexagonal crystal structure while both TiAl and Al_3Ti has a face-centered cubic crystal structure.

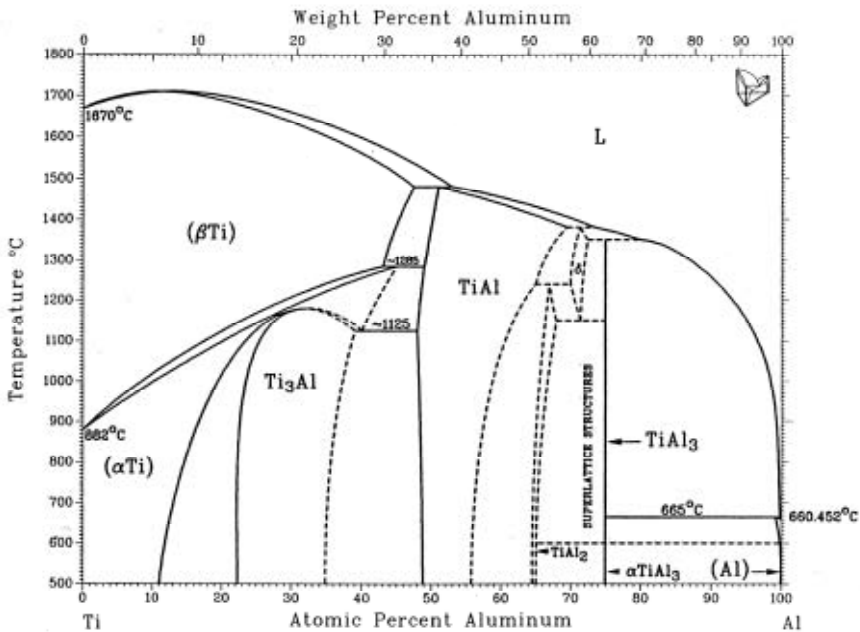


Figure 4. Binary phase diagram of Ti-Al alloys [24].

Properties such as electrical resistivity and creep resistance depend on the microstructure, as well as, the composition of Ti and Al [25,26]. At high temperatures Ti-Al forms Ti- and Al-oxides. The formation of oxides are complex and depends on phase composition, temperature, and oxygen pressure [27,28,29]. It is found that higher Al content ($>50 \text{ at}\%$) or introduction of other metals such as Cu will improve the oxidation behavior [30].

In Paper I it is shown that Ti-Al alloys play the role as binding phases and are of importance for the density and adhesion of the coatings.

3. Deposition of Thick Coatings

This section describes thermal spray, a family of established industrial techniques, which deposit coatings of thicknesses around 100 μm . These techniques utilize thermal energy to melt and soften particles, which are then accelerated (sprayed) by process gases towards a substrate. Powder, wire or rods are the most used feed stock for thermal spray, however, gas and liquids can also be utilized. The span of materials covers ceramics, polymers, and metals. The focus will be on high velocity oxy-fuel spray, which is the technique used in Paper I.

Thermal spray was invented in the beginning of the 1900's, but did not enter commercial use until a half century later. The thermal spray family is divided into three main spraying techniques; plasma, electric arc, and flame. *Plasma spray* creates thermal plasma (see Chapter 5) by an electric field which sustains a current as the free electrons move through the ionized gas. The heavy ions transfer kinetic energy in the gas upon collisions. The energy sources are usually dc, electric arc or RF. This is a hot spraying technique, which creates plasma temperatures exceeding 15 000 °C [31] depending on the gas character. The generated particle temperature reaches 3800 °C [31]. The high kinetic energy of the particles and high degree of melting generate coatings with a higher density and adhesion to substrate comparable to both flame and electric arc processes. Oxides will, however, always be present in plasma sprayed coatings hence *vacuum plasma* techniques have been developed.

Electric arc utilizes a direct current electric arc which is struck between two wires of spraying material (conductive) which melts. A fine distribution of molten metal droplets is transported by a high-velocity air jet which is introduced behind the intersection of the wires. The wires are continuously fed closer as the material is consumed. Unlike flame and plasma spray, the droplet cools down immediately as the droplets leave the arc zone and the substrate only get heated by sprayed particles, which enables spraying on substrates as polymers, wood, and even paper.

Flame spray was the first invented technique and is mainly used for spraying metals and alloys. The sprayed material is heated by combustion of fuel gases, most often a mix of acetylene and oxygen. The melted material is then accelerated by the expanding gas flow. Flame spray generates the lowest particle velocity of only 80 m/s before impact. The jet temperature is around 3500 K [31] and is controlled by the fuel/oxygen ratio. Either side of stoichiometry will cool the flame, but vary between oxidizing (oxygen rich) or reducing (fuel rich) of the feedstock material. The characteristic for flame sprayed coatings is a density ranging from 85 to 98 % and relatively high oxide content. Flame spray has, however, developed during the years and high velocity oxy-fuel is the flame spray technique that offers

higher gas velocities and consequently coatings with properties that differ from regular flame spraying.

3.1 High Velocity Oxy-Fuel

High velocity oxy-fuel (HVOF) uses the heat and velocity from combusted gases. The use of a combustion chamber and confined nozzles results in particle velocities at supersonic speed. With such high velocity, the HVOF process exhibits noticeable shock diamond patterns in the gas jet [32]. A drawback for HVOF is the noise level which is in the range of 125+ to 133+ dBA [31]. The high particle velocity generates coatings with high density and excellent adhesion. The particle temperature is lower than for plasma spray, which reduces the melting, decomposition and oxidation. Figure 5 shows a schematic of a high velocity oxy-fuel gun with its combustion chamber connected with a confined nozzle. The combustion chamber is air or water cooled to prevent oxidation of the gun components. Oxidation would be damaging for the spraying process as it reduces the cooling effect further causing powder build-up and the nozzle to melt. The powder is borne by a carrier gas and fed into the nozzle. Common gases are hydrogen, propane, kerosene or acetylene mixed with oxygen. Different shapes of the nozzle create different shapes of the spray pattern.

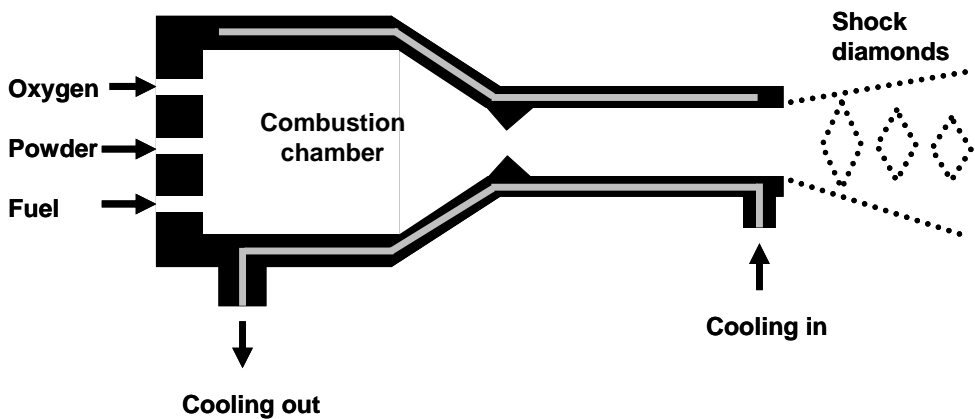


Figure 5. Schematic of a High Velocity Oxy-Fuel gun.

Ti₂AlC coatings have been deposited with HVOF and characterized in Paper I. A mix of hydrogen and oxygen gas was used to spray Ti₂AlC (MAXTHAL™ 211) powder.

3.1.1 The effect of gas and powder parameters

The spraying process is dependent on several parameters, see Figure 6. Two main ingredients are the powder and gas parameters. They affect the temperature and velocity of the spraying particles. The particle temperature and velocity will determine the characteristics of the coating such as adhesion, porosity, and content of unmelted particles and oxides [33]. The type of gases and the ratio between them will affect the gas temperature. The gas velocity in combination with the energy from the spraying process plays a main role for both the particle temperature and velocity. Both gas velocity and temperature varies greatly in the spray stream, where for instance the core is hot compared to the relatively cold surrounding. There are both radial and axial gradients of the gas temperature and velocity. Therefore reported values of dwell time (the time a particle spends in the flame) and temperatures are reported as average values for the distributions. Longer dwell time, in general, results in higher concentrations of oxide inclusions. Regarding the powder, the thermal and physical characteristics are important for the material, i.e. a solid particle melts slower than a porous granule.

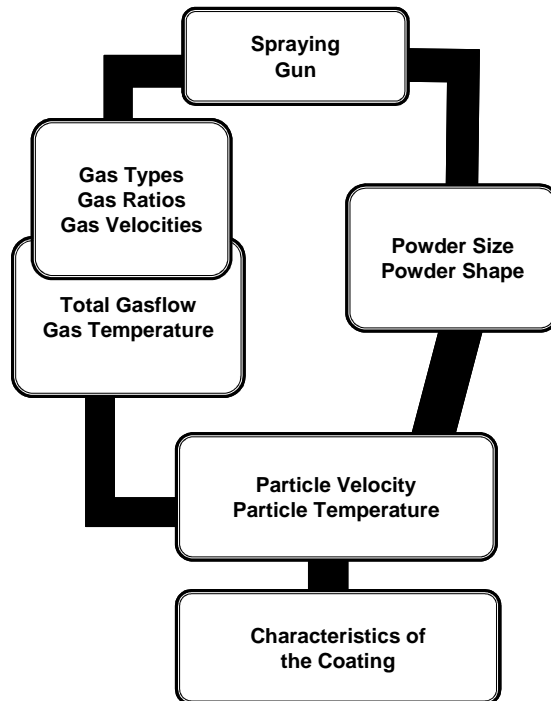


Figure 6. Illustration of the spraying process

3.1.2 Structure of Thermal Sprayed Coatings

A coating is built up by molten or heated particles that spread out and solidify very fast upon impact, so called splats [34], see Figure 7. The fast cooling rate yields formation of amorphous and metastable phases. The build-up of splats may yield a lamellar microstructure and often a very rough surface which for certain applications are be machined off. The substrate surface is sand-blasted to create a rough surface in which the splats can hook on to and create a good adhesion which mainly has a mechanical character rather than chemical [35]. The degree of melting of the particles affects the splat formation and determines the cohesion and porosity of the coating.

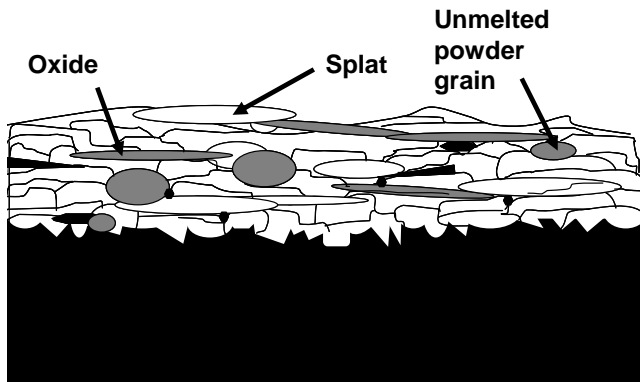


Figure 7. Schematic cross section of a thermal sprayed coating.

Porosity leads to poor cohesion within the coating, low wear resistance, low hardness and high corrosion rate. Open porosity means that a corroding agent can reach the substrate. On the other hand the porosity can be utilized to produce oil-impregnated coatings and is desired for thermal barrier coatings (TBC) to increase the thermal properties.

Oxides are present in most thermal sprayed coatings. The oxides are created during spraying when heated particles and the surface of the coating interact with the surrounding and can often be seen as dark elongated strings parallel to the substrate. Oxides have a high hardness and therefore often contribute to the average hardness of the coating and also cause brittleness. Because of this, oxides are most of the times not wanted but there are cases where oxides are desired because they increase the wear resistance or lower the thermal conductivity.

4. Synthesis of Thin Films

This section describes deposition techniques, which utilizes vapor of either molecules or atoms to grow thin films of $\sim 1\mu\text{m}$. The deposition rate depends on the technique but is in general slower than thermal spray processes. The focus in this Thesis is on magnetron sputtering, which is the technique used in Paper II.

Two main groups of deposition techniques are *chemical vapor deposition* (CVD) and *physical vapor deposition* (PVD). CVD utilizes volatile gases as starting material which react at the substrate surface to grow the coating at thermal equilibrium. This technique offers deposition of complicated geometries at high rate. Disadvantages are the use of high substrate temperature which limits the choice of substrate material, and some of the gases used are hazardous. In comparison, PVD make use of vaporization of solid material that condenses on the substrate surface. It can only deposit line-on sight, but operates at much lower temperatures than CVD. The low temperature and low pressure offers deposition far from thermal equilibrium and therefore potential growth of metastable phases. There are several ways to vaporize a solid material. *Pulsed laser deposition* (PLD) vaporizes the material with a high energy laser. *Cathodic arc deposition* and *magnetron sputtering* are two techniques that utilize plasma instead.

4.1 Sputtering

Condensation of a material must take place in a vacuum chamber to control the growth and obtain high purity of the films. The sputtering process utilizes a source of material (target) with applied negative voltage that attracts relatively heavy ions (from a plasma) and knocks out atoms from the target. These atoms are deposited one by one to grow a well-defined coating. The target can consist of a metal, a ceramic or a target of different phases and is mounted in a magnetron. In most cases argon gas is used for the plasma, but oxygen and/or nitrogen can be introduced as reactive gases to obtain ceramic coatings. This process is called reactive sputtering. The sputtering process is illustrated in Figure 8 and will be described in more detail below.

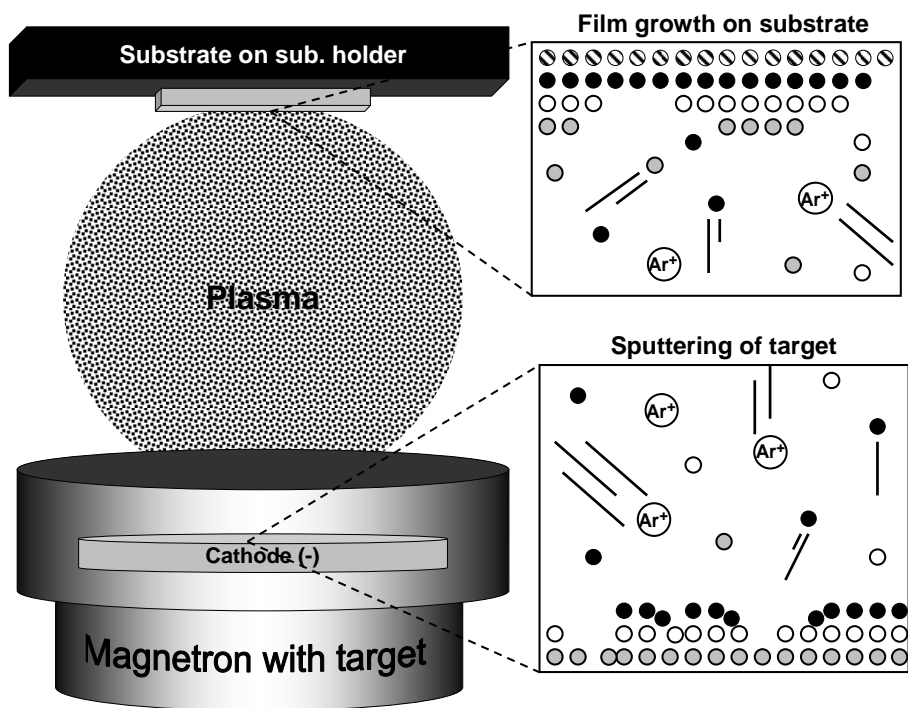


Figure 8. Schematic of the magnetron sputtering process.

In the same moment as the plasma is created the sputtering and deposition can take place. By the use of magnets, mounted behind the target, a magnetic field is applied to gather electrons. A high electron density is preferred close to the target to amplify the ionization of the plasma gas and increase the sputter rate. The argon ions must have enough momentum upon impact on the target to break bonds in the material and to transfer sufficient kinetic energy to the outgoing atoms. The now free atoms travel through the plasma of argon ions and electrons. The probability of the atom to hit argon ions depends on the pressure. Some sputtered atoms will reach the substrate without interfering with other plasma species, but most atoms will go through collisions and lose some of their kinetic energy. Many sputtered atoms will lose all of their initial kinetic energy and move randomly. These atoms are called thermalized.

Some elements are easier to sputter (knock out from the target) than others. The sputter yield states how many sputtered atoms you get from one incoming ion, in other words, the efficiency of sputtering. Values usually range from 0.1 to 10 [36]. Special interest for this Thesis is the sputtering yield of Ti, Al, and C. Sputtering with 0.5 keV Ar ions results in a

sputtering yield of 0.51 for Ti, 1.05 for Al and 0.12 for C [36]. When sputtering from an alloy target of many elements the difference in sputtering yield will be compensated for by a composition difference at the surface of the target [36]. If this can be applied to a Ti_2AlC target it would lead to a surface containing less of the elements that are easy to sputter, i.e., Al, and more of the elements that are harder to sputter, i.e., Ti and C when equilibrium is reached. As a result the out-flow from the target has a content of Ti, Al, and C representing the nominal composition of the target.

The substrate is most often heated to favor mobility of the arriving atoms. Most materials can be used as substrates as long as it can handle the temperature required for deposition. A negative voltage (bias) applied to the substrate can acquire different effects depending on its magnitude. A low voltage increases the mobility of the arriving atoms. A voltage around 100 V makes it possible to etch or sputter the surface. Higher voltage in the range of 1000 V will implant atoms into the coating or substrate.

In paper II, direct current magnetron sputtering has been utilized to deposit Ti-Al-C thin films in an ultra high vacuum (UHV) chamber.

5. Plasma physics

There are four states of matter; solid, liquid, gas, and plasma. A plasma can be described as a cloud of positive and negative charges. The overall net charge is zero, meaning that there are just as many positively charged ions as negative electrons. We have many kinds of plasma around us for instance in northern lights and the sun. Plasma is also used in many different applications and plasma physics is a well established research area. Its fascinating light is used for neon signs and energy lamps. High-energetic plasma is used for thermal spraying, as cutting tools or in disinfection processes. In this Thesis the plasma is used as a tool for depositing thin films (see section 4.1) and this chapter will bring up a few phenomenons within plasma physics and techniques for plasma analysis.

5.1 Plasma breakdown

The creation of a plasma in a gas is called plasma breakdown. For the sputtering process Ar gas is introduced into the vacuum chamber and an electric field is applied between the chamber (anode) and the target (cathode). Due to background radiation there are always a number of ions and electrons present. The electrons will accelerate towards the chamber walls and the ions are attracted to the target. When ions get close to the target, electrons from the target tunnel and neutralize the ions. Energy corresponding to the ionization energy is released. If this energy is greater than the work function for the electrons in the target it will release secondary electrons which will be transported to the plasma and ionize more argon atoms. A plasma of ions and electrons is now created.

5.2 Sheath

In the region between the plasma and a solid, in our case the chamber wall, a sheath is created. Since the electrons are much smaller and have a much higher velocity than the ions they will reach the solid surface first. The surface will get negatively charged and attract positive ions. A sheath is the region over which a potential difference occurs between the solid and the plasma. The thickness of the sheath depends on the magnitude of the potential between the negatively charged wall and the positive layer covering it. The thickness is in the range of the Debye length (λ_D), which is defined as

$$\lambda_D = \left(\frac{\epsilon_0 k T_e}{n e^2} \right)^{0.5},$$

Where ϵ_0 is the permittivity of free space, k is Boltzmann's constant, T_e is the electron temperature, n is the plasma density, and e is an elementary charge. The Debye length gives important plasma information about the behavior around inserted objects and ability to penetrate holes.

5.3 Plasma analysis

5.3.1 Langmuir probe

The Langmuir probe is an electrostatic probe used to determine the electron temperature and the plasma density (number of ions in a volume). Electron temperature is related to its velocity and is a measure of the electron energy. The electron temperature in a plasma can reach thousands of degrees. However, due to the low pressure and low mass of the electron the energy transfer is negligible.

The probe is simply one or several electrodes connected to a voltage source. The probe is inserted to the plasma, a voltage is applied with respect to ground and the current is measured. From an I-V graph (illustrated in Figure 9) one can extract the electron temperature, plasma density, floating potential, and plasma potential. When a probe without an applied voltage (or any object) is inserted in a plasma, the net voltage is slightly negative and the *probe current* is zero. It means we have no net current of electrons (I_e) or ions (I_i), $I_e = I_i$. The negative voltage is called *floating potential*, V_f , and is due to the fact that electrons have a higher mobility and will reach the electrode faster and cause a negative charge. At voltages below the floating potential, the probe draws mainly ion current (ion collects electrons from the probe) and as the probe gets saturated the curve flattens out. At the plasma potential, V_p , the probe draws mainly electron current. At voltages above the plasma potential the probe gets saturated by electrons instead and the curve flattens out.

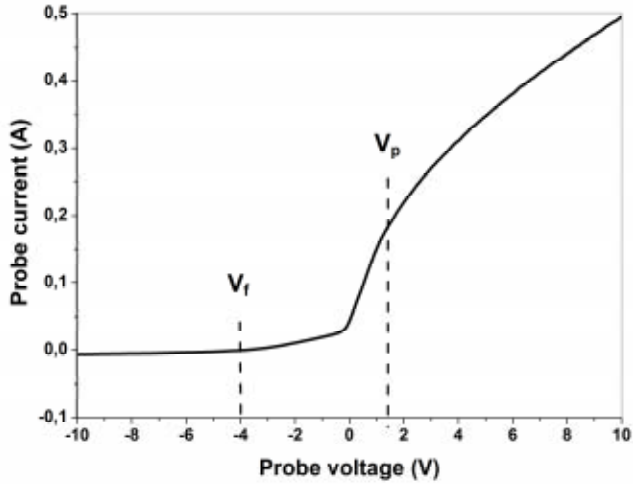


Figure 9. I-V graph for a Langmuir measurement in a plasma during sputtering from a Ti₂AlC target.

5.3.2 Mass spectrometry

Mass spectrometry is used to analyze the chemical and energy distribution of ion species. The ions can be both elemental and molecules which makes mass spectrometry useful for both inorganic and organic chemistry as well as for physics. This section focuses on mass spectrometry for plasma analysis.

The mass spectrometry technique separates ions according to their mass (m) and charge (q), called mass ratio, M .

$$M = \frac{m}{q} \quad (1)$$

The ions are first accelerated by a potential (V) giving them a specific kinetic energy (E_{kin}).

$$E_{kin} = qV = \frac{mv^2}{2} \quad (2)$$

From equation (1) and (2) the relation between mass ratio and voltage is derived.

$$V \frac{2}{v^2} = \frac{m}{q} \quad (3)$$

When scanning over a voltage range, ions are separated by mass and let through to the detector to be analyzed. The mass spectrometry equipment works under low pressure to increase the mean free path of the species. The species enters an orifice which can either be electrically floating, biased or grounded. If investigating neutral species there must be an ionization source inside the orifice. A common source would be a filament that emits electrons. Next there is an energy filter and a mass filter. The combination of energy and mass filters is required for measurements of the energy distribution for species with different masses, but also to improve the resolution for mass scans by filtering out the low energy ions. The detector consists of an electron multiplier to increase the intensity. The instrumental setup is illustrated in Figure 10.

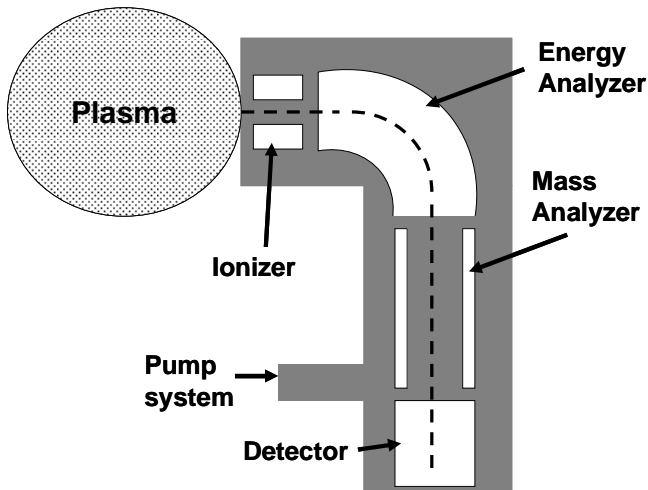


Figure 10. General principle for a mass spectrometer.

Two main spectrometers are available, either a mass energy analyzer (MEA) or a time of flight (TOF). A mass energy analyzer has separated energy and mass filters. The energy filter uses an electric field to only allow ions with a specific kinetic energy to pass through. A common mass filter is the quadrupole which consists of four cylindrical electrodes mounted

parallel to the ion path in a square array. A quadrupole is illustrated in Figure 11. A potential is applied over each diagonal pair of electrodes. The potentials are a combination of both dc and rf and are synchronized between the pairs. Ions entering the quadrupole will start to oscillate. At a specific dc and rf potential only ions with the right mass-to-charge ratio will get a limited oscillation and pass through the quadrupole without smashing into the electrodes. The velocity of the ions will not affect the amplitude of the oscillation and consequently not affect the result. The resolution is determined by the ratio between dc and rf voltage which is kept constant during the mass scan [37].

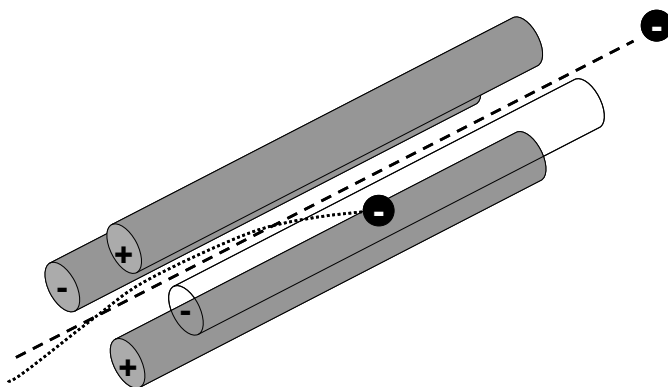


Figure 11. Schematic of a quadrupole.

A time of flight mass spectrometer utilizes the kinetic energy discussed above, see equation (2).

$$E_{kin} = \frac{mv^2}{2}$$

Ions with the same kinetic energy will separate due to mass because lighter ions will travel faster than heavier ions. The detector will then distinguish the different ions due to the time it takes for the ion to reach the detector. The peak broadening gives information about the energy distribution.

6. Comments on the Results

Here I summarize and discuss the results from the papers of this Thesis. The papers differ by the choice of deposition technique used for Ti₂AlC coatings. Paper I focuses on high velocity oxy-fuel spraying and Paper II presents synthesis by the direct current magnetron sputtering technique.

Paper I

We demonstrate how Ti₂AlC coatings can be produced by the high velocity oxy-fuel (HVOF) thermal spray technique. Ti₂AlC (MAXTHAL 211) powder was used as a source of material and the coatings were sprayed with a combustion gas of H₂ and O₂. The study also focuses on how the powder size and the total gas flow affects the microstructure as well as the phase content. We find that coatings sprayed with a relatively coarse powder of ~56 μm exhibit a high content of Ti₂AlC, which is not surprising considering that large powder melts to a smaller extent. It is, however, at the expense of a more porous coating with cracks and delaminations. When spraying with a finer powder of ~38 μm the amount of Ti₂AlC is found to range with the total gas flow of H₂ and O₂. This means that a finer powder is more sensitive to heating as the gas ratio affects the power of the flame. The coatings are dense and exhibit good adhesion to stainless steel substrates. In addition to Ti₂AlC, other phases such as TiC, and Al_xTi_y alloys are present in the coatings and their content also scales with the gas mix ratio. A model for the operating phase transformations is also suggested.

By introducing Ti₂AlC to a new area of deposition techniques there are a lot of interesting topics to continue this research within. More investigations about the mechanical properties of these coatings are needed as well as oxidation studies in different environments. Parallel to this, fundamental studies to receive a deeper understanding on the phase transformations during spraying would be of interest to be able to fine-tune the process.

Paper II

In this study we have investigated a new way of utilizing a previously reported, but not fully described deposition technique for MAX phase thin films. By using one compound target for d.c. magnetron sputtering instead of three elemental targets the aim is to simplify the sputtering process and make up-scaling possible for industrial purposes. The on-set for my study is the phenomenon on a non-conserved composition between the compound target and resulting film.

Ti-Al-C thin films were sputtered on Al₂O₃ 0001 substrates at temperatures between ambient and 1000 °C and at target-to-substrate distances of 6 or 9 cm. Sputtering from a compound target was shown to yield film compositions other than the nominal content of the target. Especially the carbon content was remarkably high exceeding even the content of Ti. This is partly explained by differences in transport where a substantial part of the carbon was shown to exhibit a relatively high kinetic energy when reaching the substrate surface. It is also suggested to be an effect of gas-phase scattering processes in combination of the angular distribution of the sputtered species. The Al content was affected by the substrate temperature around 700 °C due to its high vapor pressure. It is suggested that if the Ti/C ratio is correct Ti₂AlC can be synthesized at higher temperatures even with Al-poor contents. This was also demonstrated by co-sputtering with an additional Ti target which yielded a Ti₂AlC thin film. The possibility of employing a compound target with a composition that compensates for the apparent Ti and Al loss during deposition for MAX-phase growth is a topic for future investigation.

The microstructure of the Ti₂AlC film showed two kinds of grains with different out-of-plane orientations which both seems to have taken part in a solid state reaction with the Al₂O₃ substrate. Further investigation for the understanding of this reaction would be interesting, as would any reaction with other substrate materials. As the reaction includes high contents of oxygen, future studies of oxygen incorporation in a range of MAX phases are of interest as has been recently been reported by Rosén et al. for the case of Ti₂AlC [38].

References

- [1] W. Jeitschko, H. Nowotny, *Montashefte für Chemie* **98** (1967) 328
- [2] M.W. Barsoum, T. El-Raghy, *Journal of the American Ceramic Society* **79** (1996) 1953
- [3] N.V. Tzenov, M.W. Barsoum, *Journal of the American Ceramic Society* **83** (2000) 825
- [4] J.D. Hettinger, S.E. Lofland, P. Finkel, T. Meehan, J. Palma, K. Harrell, S. Gupta, A. Ganguly, T. El-Raghy, M.W. Barsoum, *Physical Review B* **72** (2005) 115120
- [5] S. Amini, M.W. Barsoum, T. El-Raghy, *Journal of the American Ceramic Society* **90** (2007) 3953
- [6] J.J. Nickl, K.K. Schweitzer, P. Luxenberg, *Journal of the Less-Common Metals* **26** (1972) 335
- [7] T. Seppänen, J.-P. Palmquist, P.O.Å. Persson, J. Emmerlich, J. Molina, J. Birch, U. Jansson, P. Isberg, L. Hultman, *Proceedings of the 53rd Annual Meeting of the Scandinavian Society for Electron Microscopy* **142** (2002) ISSN: 1455
- [8] M.A. Pietzka, J.C. Schuster, *Journal of Phase Equilibria* **15** (1994) 392
- [9] Y. Zhou, Z. Sun, *Physical Review B* **61** (2000) 12570
- [10] Z. Sun, D. Music, R. Ahuja, S. Li, J.M. Schneider, *Physical Review B* **70** (2004) 092102
- [11] Y.C. Zhou, X.H. Wang, *Materials Research Innovations* **5** (2001) 87
- [12] M.W. Barsoum, D. Brodtkin, T. El-Raghy, *Scripta Materialia* **36** (1997) 535
- [13] B. Manoun, R.P. Gulve, S.K. Saxena, S. Gupta, M.W. Barsoum, C.S. Zha, *Physical Review B* **73** (2006) 024110
- [14] M.W. Barsoum, M. Ali, T. El-Raghy, *Metallurgical and Materials Transaction A* **31** (2000) 1857
- [15] O. Wilhelmsson, J.-P. Palmquist, *Applied Physics Letters* **85** (2004) 1066
- [16] X.H. Wang, Y.C. Zhou, *Corrosion Science* **45** (2003) 891
- [17] *Alumina as a Ceramic Material*, W. H. Gitzen [Ed.], The American Ceramic Society, Westerville, Ohio (1970) ISBN 0-916094-46-4
- [18] M.W. Barsoum, *Progress in Solid State Chemistry* **28** (2000) 201
- [19] M. Sundberg, G. Malmqvist, A. Magnusson, T. El-Raghy, *Ceramics International* **30** (2004) 1899
- [20] *Handbook of Refractory Carbides and Nitrides*, Hugh O. Pierson, Noyes Publications, Westwood, New Jersey, USA ISBN: 0-8155-1392-5
- [21] W.S. Williams, *Progress in Solid State Chemistry* **6** (1971) 57
- [22] H. Högberg, J. Birch, M. Oden, J.O. Malm, L. Hultman, U. Jansson, *Journal of Materials Research* **16** (2001) 1301
- [23] F. Appel, R. Wagner, *Materials Science and Engineering* **R22** (1998) 187

-
- [24] Binary Alloy Phase Diagram, J.L. Murray, American Society for Metals, Metals Park Ohio, USA 1986
- [25] D. Veeraraghavan, V.K. Vasudevan, *Materials Science and Engineering A* **192/193** (1995) 950
- [26] M.F. Bartholomeusz, M.A. Cantrell, J.A. Wert, *Materials Science and Engineering A* **201** (1995) 24
- [27] A. Rahmel, P.J. Spencer, *Oxidation of Metals* **35** (1991) 53
- [28] V. Maurice, G. Despert, S. Zanna, P. Josso, M.-P. Bacos, P. Marcus, *Acta Materialia* **55** (2007) 3315
- [29] K. Kovács, V.K. Josepovits, G. Kiss, H. Zillgen, P. Deák, *Physica Status Solidi* **193** (2002) R1
- [30] J. Lee, W. Gao, M. Hodgson, *International Journal of Modern Physics B* **17** (2003) 1711
- [31] Handbook of thermal spray technology, J.R. Davis, American Society for Metals, Metals Park, Ohio, USA (2005) ISBN 0-87170-795-0
- [32] A. Dolatabadi, V. Pershin, J. Mostaghimi, *Journal of Thermal Spray Technology* **14** (2005) 91
- [33] M. Li, P.D. Christofides, *Journal of Thermal Spray Technology* **13** (2004) 108
- [34] V.V. Sobolev, *Materials Letters* **36** (1998) 123
- [35] C.R.C. Lima, J.M. Guilemany, *Surface and Coatings Technology* **201** (2007) 4694
- [36] *Materials Science of Thin Films*, M. Ohring, Academic Press, London UK 2002
- [37] J.P. Eberhart, *Structural and Chemical Analysis of Materials*, Wiley, (1991)
ISBN: 0471929778
- [38] J. Rosén, P.O.Å. Persson, M. Ionescu, A. Kondyurin, D.R. McKenzie, M.M.M. Bilek, *Applied Physics Letters* **92** (2008) 064102